Theory of ferromagnetic resonance driven by the combined action of spin-transfer torque and voltage-controlled magnetic anisotropy

C. Gonzalez-Fuentes,* C. Garcia, P. Landeros, and R. A. Gallardo
Departamento de Física, Universidad Técnica Federico Santa María, Avenida España 1680, 2390123 Valparaíso, Chile
(Received 20 June 2017; revised manuscript received 3 October 2017; published 27 November 2017)

An analytical study of the spectral line shape of ferromagnetic resonance (FMR) detected by spin rectification effect and driven by the combined action of spin-transfer torque (STT) and voltage-controlled magnetic anisotropy (VCMA) is developed. The system under consideration consists of a magnetic tunnel junction (MTJ). Explicit expressions for the symmetric and asymmetric components of the rectified voltage are derived, where the role of the VCMA, in-plane STT, and field-like torque is clearly identified and discussed. Typical geometrical configurations are particularly analyzed and compared with recent experimental results. The analytical findings show that the change of sign in the FMR response upon reversal of the magnetization is completely due to VCMA. By distinguishing in-plane, out-of-plane, and full magnetization reversal processes, it is shown that the VCMA induces a change of sign in the symmetric part for the in-plane and out-of-plane magnetization reversal, while the asymmetric part change its sign under a full and in-plane reversion of the magnetization. Explicit expressions of the symmetric and asymmetric contributions of the spectral line shape allow us to detect under what conditions the STT and VCMA can increase or decrease the FMR spectral line shape. The proposed theory allows access to a better understanding of the physics behind ferromagnetic resonance phenomena, promoting potential applications in STT+VCMA-based MTJs.

DOI: 10.1103/PhysRevB.96.174440

I. INTRODUCTION

The manipulation of magnetization with spin polarized currents through spin-transfer torque [1–3] plays a central role in the field of spintronics. Besides its intrinsic interest as physical phenomenon, STT is also the basis of new classes of emerging technologies such as magnetoresistive random access memories, nonvolatile logic chips, and STT self-oscillators [4–8]. Despite these important achievements there still persists significant technological disadvantages, for instance the high electric current densities needed to manipulate the magnetization, which is unavoidably accompanied by high power consumption and Joule heating [9]. Therefore, new ways to control the magnetization dynamics are of great interest for the spintronics community. The control of magnetic anisotropy by electric fields has been recently proposed as an alternative method to manipulate the magnetization state [9–23]. To use electric fields rather than electric currents greatly reduces Ohmic losses and thereby improves the performance of spintronic devices. In this context, the VCMA phenomenon has been extensively studied on ferromagnetic/insulator junctions [9,19–23], where the interfacial perpendicular magnetic anisotropy is modified by the application of a voltage perpendicular to the ferromagnetic (FM) film. On the other side, FM/insulator interfaces in MTJs have been also widely employed to study the role of STT in the magnetization dynamics [24–27]. Therefore, both VCMA and STT effects can influence the dynamic behavior of the magnetization provided the lateral dimensions of the MTJ are small enough (order of tens of nanometers) to have an appreciable STT. Indeed, it was recently demonstrated that both spin-transfer torque and voltage-controlled magnetic anisotropy torques are equally important, since both can contribute either to magnetization switching [28] or FMR response [18].

The suitable experimental technique to study the magnetization dynamics on micro- and nanostructured MTJs is the FMR spectroscopy, where the output signal or spectral line shape is detected by the spin rectification effect [29,30], which consists of the homodyne rectified voltage arising from the rf applied current and rf tunneling magnetoresistance. It is well established that while the in-plane component of STT is proportional to the symmetric part of the FMR peak, the field-like torque (FLT) component contributes to the antisymmetric one [31,32]. However, in the case of VCMA-induced FMR, some conclusions cannot be directly obtained as in the case of STT. For instance, it has been reported that VCMA may affect both symmetric and asymmetric components of the output signal depending on the direction of the applied magnetic field [18,22]. Moreover, VCMA presents some peculiarities like the change of sign of the rectified voltage upon reversal of the external field [18,22]. To date, there is a lack of a general theoretical framework that allows identifying and quantifying the role of the combined action of STT and VCMA on the FMR response in MTJs. This is not only important from the physics point of view but also for potential applications of the MTJs as microwave detectors [33], where the optimization of the spin rectification voltage is crucial.

In this paper an analytical description of the VMCA+STT-induced FMR phenomenon is developed. Explicit expressions for symmetric and asymmetric contributions of the FMR line shape are derived, where the role of the VCMA, FLT, and in-plane STT (ipSTT) are clearly identified and compared with recent experimental measurements.

II. THEORETICAL DESCRIPTION

In order to take into account a generalized geometry of the system, a reference frame (x,y,z) is considered (see Fig. 1).

*claudio.gonzalezfu@usm.cl

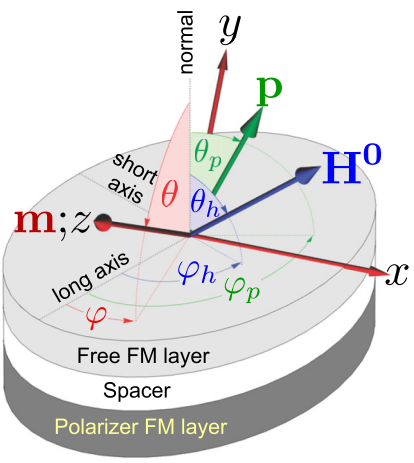

FIG. 1. Geometry considered in the theoretical description. The reference system (x,y,z) is defined in such a way that the equilibrium magnetization of the free layer points along the z axis and x lies in the plane. Angles φ, φ_h, and φ_p represent the azimuthal angles of the equilibrium magnetization, external field, and the polarizer, respectively, measured from the long axis. In the same way, angles θ, θ_h, and θ_p are the polar angles measured from the normal.

By controlling angles φ and θ, which define the equilibrium orientation of the magnetization, as well as φ_p and θ_p, which represents the magnetic orientation of the polarizer $\mathbf{p}$, any geometrical configuration can be theoretically addressed. The time evolution of the free layer magnetization is described by the Landau-Lifshitz-Gilbert (LLG) equation plus STT terms: $\dot{\mathbf{m}} = -\gamma\mathbf{m}\times[\mathbf{H}^{\mathrm{e}} - \frac{\alpha}{\gamma}\dot{\mathbf{m}} - \beta_{\shortparallel}\mathbf{m}\times\mathbf{p} - \beta_{\perp}\mathbf{p}]$. Here the dot denotes the time derivative, γ is the gyromagnetic ratio, α is the Gilbert damping, $\beta_{\shortparallel}\mathbf{m}\times\mathbf{p}$ is the ipSTT also known as the nonadiabatic or Slonczewski STT, and $\beta_{\perp}\mathbf{p}$ is the FLT, also known as the adiabatic or out-of-plane STT. The electric current is positive for electrons flowing from the free to the polarizer FM layer. Vector $\mathbf{m}$ represents the unit free layer magnetization, normalized to the saturation magnetization M_{s}, and $\mathbf{H}^{\mathrm{e}}$ is the effective field, which contains the driving field due to an rf voltage. By writing $\beta'_{\shortparallel,\perp} = [d(\beta_{\shortparallel,\perp})/dI]$ [31], the LLG+STT equation can be written as

$$\dot{\mathbf{m}} = -\gamma\mathbf{m}\times\left[\mathbf{H}^{\mathrm{e}} - \frac{\alpha}{\gamma}\dot{\mathbf{m}} - I(t)(\beta'_{\shortparallel}\mathbf{m}\times\mathbf{p} - \beta'_{\perp}\mathbf{p})\right], \quad (1)$$

where $I(t)$ represents the oscillating current injected into the MTJ. This current generates an Oersted field, which may be significant inside the free layer, nevertheless the vector sum of the Oersted field over a resonant mode is null for the macrospin model [34], so that this field is not included in the analysis. The voltage will make a periodic modulation over time on the perpendicular magnetic anisotropy field, where the normal component of the anisotropy field can be expressed as [18,19]

$$H_{\mathrm{s}} = H_{\mathrm{s}}^0 - \frac{dH_{\mathrm{s}}}{dV}\left(V_{\mathrm{dc}} + V_{\mathrm{rf}}^0 e^{i\omega t}\right), \quad (2)$$

where H_{s}^0 is the magnitude of the unperturbed anisotropy field, and V_{dc} and V_{rf}^0 are the dc and rf components of the voltage, respectively. In this expansion, dH_{s}/dV is assumed positive, to be in agreement with the reported experimental evidence [10,18,19] showing that the magnitude of H_{s} increases when positive charges accumulate at the interface between free layer and spacer. Here dH_{s}/dV represents the efficiency of the VCMA effect. With respect to its sign, it has been found that H_{s} increases when the free FM layer is charged positively [18,19], so that dH_{s}/dV is positive. Moreover, Zhu *et al.* [18] found that dH_{s}/dV is practically constant over the full range of voltages employed. The flowing current through the MTJ can be treated like the leakage current of a parallel plate capacitor [35]. Therefore, the complex impedance may be approximated by that of a parallel RC circuit, i.e., $Z = R/(1+i\omega RC)$, where C is the capacitance. In the approximation of an infinite parallel plate capacitor, the capacitance is given by $C = A\varepsilon/d$. Taking the value of the MgO dielectric constant as [36] $\varepsilon = 8.76\times10^{-11}$ Fm^{-1}, $d\sim$ nm, and typical values of resistance-area product of tunnel junctions [18,21] $\sim10^{-9}\Omega\,\mathrm{m}^2$, it is obtained that the product ωRC is $\sim10^{-2}$. Then, it may be assumed that $Z\approx R$, so that microwave voltage and current are approximately in phase. Thus $H_{\mathrm{s}} = H_{\mathrm{s}}^0 - \beta'_{\mathrm{v}}(I_{\mathrm{dc}} + I_{\mathrm{rf}}^0 e^{i\omega t})$, where it has been defined

$$\beta'_{\mathrm{v}} = \frac{dH_{\mathrm{s}}}{dI} = \frac{1}{R}\frac{dH_{\mathrm{s}}}{dV}. \quad (3)$$

The term β'_{v} is the current efficiency of the VCMA effect. One can note that terms $\beta'_{\shortparallel}$ and $\beta'_{\perp}$ defined in Eq. (1), and β'_{v} defined in Eq. (3), have the same units.

Under the linearization approach, the unit magnetization of the free layer can be written as $\mathbf{m} = \hat{z} + \mathbf{m}_{\perp}$, with $\mathbf{m}_{\perp} = m_x(t)\hat{x} + m_y(t)\hat{y}$ being the dynamic magnetization. By writing $m_{x,y}(t) = m_{x,y}^0 e^{i\omega t}$ and assuming $\alpha^2 + 1 \approx 1$, the LLG+STT equation of motion (1) can be separated into two coupled equations:

$$(\Omega_{xy} - i\omega)m_x^0 + (\Omega_{yy} - i\alpha\omega)m_y^0 = T_x, \quad (4)$$

$$(\Omega_{xx} + i\alpha\omega)m_x^0 + (\Omega_{yx} - i\omega)m_y^0 = T_y. \quad (5)$$

Here $T_x = \gamma I_{\mathrm{rf}}^0[\beta'_{\shortparallel}p_x + \beta'_{\perp}p_y + (\beta'_{\mathrm{v}}/2)\sin 2\theta]$ and $T_y = \gamma I_{\mathrm{rf}}^0(-\beta'_{\perp}p_x + \beta'_{\shortparallel}p_y)$. Elements $\Omega_{\eta\eta'}$ have frequency units and explicit expressions can be found in the Appendix. Also, $p_x = -\sin\theta_p\sin(\varphi-\varphi_p)$, $p_y = -\sin\theta_p\cos(\varphi-\varphi_p)\cos\theta + \sin\theta\cos\theta_p$, and $p_z = \sin\theta\sin\theta_p\cos(\varphi-\varphi_p) + \cos\theta\cos\theta_p$. By using Cramer's rule, the normalized dynamic components are

$$\begin{pmatrix} m_x(t) \\ m_y(t) \end{pmatrix} = \frac{e^{i\omega t}}{\omega^2 - \omega_{\mathrm{r}}^2 - i\lambda\omega}\begin{pmatrix} A_x - iS_x\omega \\ A_y - iS_y\omega \end{pmatrix}, \quad (6)$$

where $\omega_{\mathrm{r}}^2 = \Omega_{xy}\Omega_{yx} - \Omega_{yy}\Omega_{xx}$ and $\lambda = (\Omega_{xx} - \Omega_{yy})\alpha - 2\gamma I_{\mathrm{dc}}\beta'_{\shortparallel}p_z$. Here it is easy to see that ω_{r} is the resonance frequency, while λ is the FMR linewidth [37]. Also, $A_x = \Omega_{yy}T_y - \Omega_{yx}T_x$, $A_y = \Omega_{xx}T_x - \Omega_{xy}T_y$, $S_x = -T_x$, and $S_y = -T_y$.

In a typical experimental setup to electrically detect FMR, a microwave and a dc current are simultaneously injected into the sample through a bias tee [19,31,38]. The temporal average of the measured voltage will depend on the total current $I(t)$ and the electrical resistance R, which in turn depends directly on the relative angle $\zeta(t)$ between the magnetization and the polarizer. By writing $I(t) = I_{\mathrm{dc}} + I_{\mathrm{rf}}(t)$ and

$\zeta(t) = \zeta_0 + \delta\zeta(t)$, the change on the averaged voltage is given by

$$\delta V = \left\langle \left.\frac{\partial V}{\partial \zeta}\right|_{\zeta_0} \delta\zeta(t) + \left.\frac{\partial V}{\partial I}\right|_{I_{\rm dc}} I_{\rm rf}(t) + \frac{1}{2}\left.\frac{\partial^2 V}{\partial I^2}\right|_{I_{\rm dc}} I_{\rm rf}(t)^2 + \left.\frac{\partial^2 V}{\partial I \partial \zeta}\right|_{I_{\rm dc},\zeta_0} I_{\rm rf}(t)\delta\zeta(t) + \frac{1}{2}\left.\frac{\partial^2 V}{\partial \zeta^2}\right|_{\zeta_0} \delta\zeta(t)^2 \right\rangle. \quad (7)$$

Since both $\delta\zeta(t)$ and $I_{\rm rf}(t)$ have a periodic time dependence, both the first and second terms average to zero. The third term arises from the nonlinearity of the I-V curve and gives rise to nonresonant background in δV, so that it is neglected. The last two terms of Eq. (7) are the most relevant, because they are proportional to the amplitude of the magnetization precession and hence are key to detect the FMR signal. In a typical MTJ, the expression for the voltage is written as $V = R(I,\zeta)I$, where R is the tunnel magnetoresistance. Recalculating Eq. (7), one finds

$$\delta V = \left[\left(\left.\frac{\partial^2 R}{\partial\zeta\partial I}\right|_{I_{\rm dc},\zeta_0}\right) I_{\rm dc} + \left.\frac{\partial R}{\partial\zeta}\right|_{\zeta_0}\right]\langle I_{\rm rf}(t)\delta\zeta(t)\rangle + \frac{1}{2} I_{\rm dc}\left(\left.\frac{\partial^2 R}{\partial\zeta^2}\right|_{\zeta_0}\right)\langle\delta\zeta(t)^2\rangle. \quad (8)$$

In the model it is assumed that $I_{\rm dc}$ is of the same order of magnitude as $I^0_{\rm rf}$, so that the terms proportional to $I_{\rm dc}$ in Eq. (8) are neglected. Note that the last term in Eq. (8) may give origin to rectified voltage by anisotropic magnetoresistance (AMR) [39], however, provided that in this case $I_{\rm dc}$ is small and the tunneling magnetoresistance is much larger than AMR, this term is dropped out [39,40]. Thus, the change on the averaged voltage becomes

$$\delta V = \partial R/\partial\zeta|_{\zeta_0}\langle I_{\rm rf}(t)\delta\zeta(t)\rangle. \quad (9)$$

For the tunnel magnetoresistance, the Slonczewski expression [41] $R = R_0/(1 + P^2\cos\zeta)$ is assumed, where P is the polarization factor, and R_0 is the electrical resistance at $\zeta = 90^\circ$. On the other side, one can note that $\cos[\zeta(t)] = \mathbf{m}(t)\cdot\mathbf{p}$ and since $\delta\zeta(t)$ is a perturbation, it can be expanded up to first order in the dynamic magnetization components, this is $\delta\zeta(t) = -[m_x(t)p_x + m_y(t)p_y]/\sin\zeta_0$, where ζ_0 is the equilibrium value of ζ and $m_{x,y}(t)$ are given in Eq. (6). Thus, Eq. (9) becomes

$$\delta V = \frac{R_0 P^2 I^0_{\rm rf}}{2(1 + P^2\cos\zeta_0)^2} L_s, \quad (10)$$

where L_s is a dimensionless function that defines the "line shape" of the FMR response and is given by

$$L_s = \frac{\mathcal{A}[(\omega/\omega_{\rm r})^2 - 1] + \mathcal{S}(\lambda/\omega_{\rm r})(\omega/\omega_{\rm r})^2}{[(\omega/\omega_{\rm r})^2 - 1]^2 + (\lambda/\omega_{\rm r})^2(\omega/\omega_{\rm r})^2}. \quad (11)$$

Here $\mathcal{S}$ and $\mathcal{A}$ correspond to the *symmetric* and *asymmetric* components of the FMR response, where $\mathcal{S} = -(S_x p_x + S_y p_y)/\omega_{\rm r}$ and $\mathcal{A} = -(A_x p_x + A_y p_y)/\omega_{\rm r}^2$. Thus,

$$\mathcal{S} = \frac{\gamma I^0_{\rm rf}}{\omega_{\rm r}}\left[\beta'_{\shortparallel}\left(1 - p_z^2\right) + \beta'_{\rm v} p_x \sin\theta\cos\theta\right] \quad (12)$$

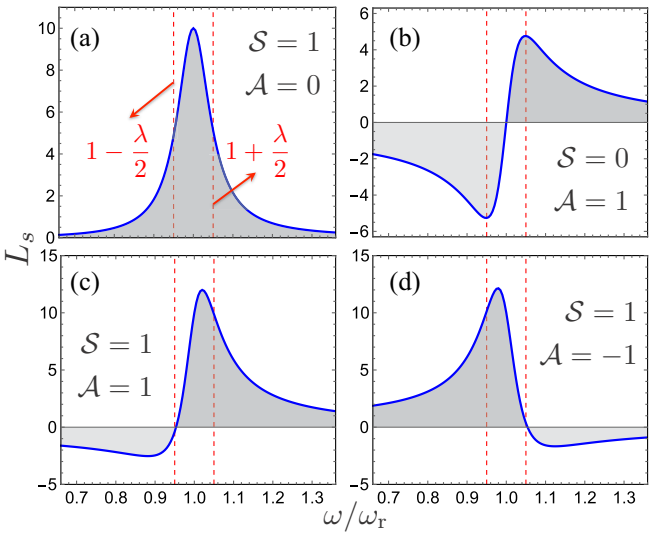

FIG. 2. (a) and (b) show the completely symmetric and asymmetric line shape, respectively. (c) and (d) represent the sum of a completely symmetric and asymmetric by line shape with equal and opposed signs, respectively. Red vertical dashed lines denote the frequency range of width $\lambda = 0.1\omega_{\rm r}$.

and

$$\mathcal{A} = -\frac{\gamma I^0_{\rm rf}}{\omega_{\rm r}^2}\left[\gamma\beta'_{\rm v} H_{xx} p_y \sin\theta\cos\theta + \gamma\beta'_{\perp}\left(H_{xx}p_y^2 + H_{yy}p_x^2\right) - \gamma\beta'_{\shortparallel}(H_{yy} - H_{xx})p_x p_y\right]. \quad (13)$$

Here the second order terms on α, $\beta'_{\perp,\shortparallel,\rm v}$ have been neglected. Also, since H_{xy} is negligible for typical elliptical structures [see Eq. (A2c) in the Appendix], the terms proportional to it have been dropped out. The elements $H_{\eta,\eta'}$ are given in the Appendix.

The line-shape function L_s represents the main result of this paper. Functions $\mathcal{S}$ and $\mathcal{A}$ explicitly contain the STT and VCMA dependence and therefore the role of both STT and VCMA torques can be directly quantified once the spectral FMR line shape is experimentally obtained.

III. RESULTS AND DISCUSSION

Knowing the relative magnitude of $\mathcal{A}$ in comparison with $\mathcal{S}$, as well as their respective signs, gives out valuable qualitative information of L_s around $\omega_{\rm r}$. For instance, in Fig. 2(a) one can see the case of a completely symmetric line shape, while in Fig. 2(b) a completely asymmetric case is shown. Figures 2(c) and 2(d) show the sum of a completely symmetric and asymmetric L_s with equal and opposed signs, respectively.

In the following sections typical geometries, which have been studied in recent experimental setups, will be discussed. For simplicity, the polarizer is in-plane and parallel to the long easy axis, i.e., $\theta_p = 90^\circ$ and $\varphi_p = 0$.

A. Magnetization perpendicular to the short axis

In this case the in-plane component of the field is applied along the long axis ($\varphi_h = 0,180^\circ$), while the out-of-plane component of the external field will induce an out-of-plane configuration of the equilibrium magnetization. According to

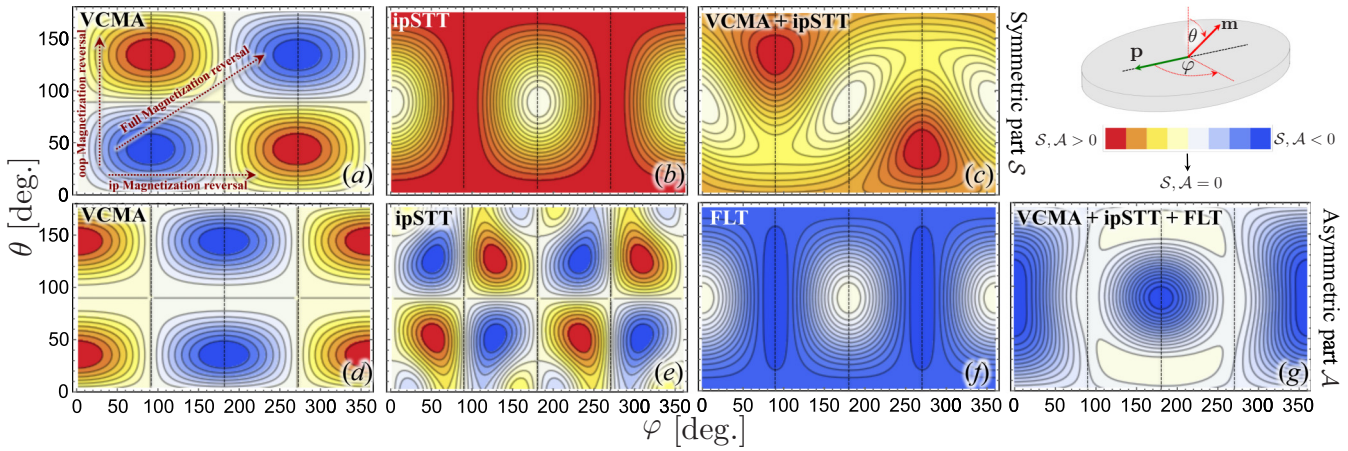

FIG. 3. Angular dependence of functions $\mathcal{S}$ [(a)–(c)] and $\mathcal{A}$ [(d)–(g)], which are represented by the color code. Arbitrary units have been used for function $\beta'_{\text{II},\perp,\text{v}}$. In (a) and (d) [(b) and (e)] just the influence of VCMA (ipSTT) is taken into account, while in (f) only the role of the FLT is considered. The combined action of the VCMA and ipSTT is shown in (c), while in (g) the combined action of VCMA, ipSTT and FLT is considered. In (a), the in-plane (ip), out-of-plane (opp), and full magnetization reversal processes are illustrated. Here it is assumed that β'_{II}, $\beta'_{\perp}$, and β'_{v} have the same order of magnitude.

Fig. 1, in this configuration the magnetization is oriented in the plane spanned by the long axis and the film's normal; the azimuthal angle is given by $\varphi = 0$ or 180°. Since $p_x = 0$, $p_y = -\cos\theta\cos\varphi$, and $p_z = \sin\theta\cos\varphi$, the factors $\mathcal{S}$ and $\mathcal{A}$ in Eqs. (12) and (13) are reduced to

$$\mathcal{S} = \frac{\gamma I^0_{\text{rf}}}{\omega_{\text{r}}}\beta'_{\text{II}}\cos^2\theta, \tag{14a}$$

$$\mathcal{A} = \frac{\gamma^2 I^0_{\text{rf}}}{\omega^2_{\text{r}}}H_{xx}(\beta'_{\text{v}}\cos\varphi\sin\theta - \beta'_{\perp})\cos^2\theta. \tag{14b}$$

Despite the simple structure of Eqs. (14a) and (14b), useful features of both symmetric and asymmetric parts can be readily identified. First, under the absence of STT ($\beta'_{\text{II}} = \beta'_{\perp} = 0$) the line shape L_s will be always asymmetric, which has been experimentally confirmed [22]. Furthermore, if $\mathcal{A}$ is dominated by the VCMA, the line shape will change its sign when the azimuthal angle φ changes from 0 to 180° (ip magnetization reversal) and this modulation in the line shape is in full concordance with recent experimental results [18,22]. In addition, if the Zeeman energy dominates, the out-of-plane angular dependence of the VCMA signal goes as $\sin\theta\cos^2\theta$, which has been also reported [19].

B. Magnetization perpendicular to the long axis

Here the in-plane component of the external field is applied along the short axis $\varphi_h = \pm 90°$, in such a way that the magnetization lies in the plane perpendicular to the long axis, provided the external field is able to overcome the uniaxial anisotropy field for doing this configuration stable. The angle φ is $\pm 90°$ and therefore $p_x = -\sin\varphi$ and $p_y = p_z = 0$. Thus, the symmetric and asymmetric functions are

$$\mathcal{S} = \frac{\gamma I^0_{\text{rf}}}{\omega_{\text{r}}}(\beta'_{\text{II}} - \beta'_{\text{v}}\sin\theta\cos\theta\sin\varphi), \tag{15a}$$

$$\mathcal{A} = -\frac{\gamma I^0_{\text{rf}}}{\omega^2_{\text{r}}}\gamma H_{yy}\beta'_{\perp}. \tag{15b}$$

In this case, it is observed that VCMA influences only the symmetric part, while the STT influences both $\mathcal{S}$ and $\mathcal{A}$. Again, the VCMA torque changes the sign of the line shape for an ip magnetization reversal, i.e., φ changes from 90° to −90°. This behavior has been experimentally observed by Shiota *et al.* in CoFeB/MgO-based tunnel junctions [22]. From Eq. (15a), one can see that the increasing or decreasing of the output signal is closely related to the change of sign induced by VCMA. This is a relevant result in this paper, since it allows a quantification of both STT and VCMA contributions.

C. General angular dependence

The angular dependence of both symmetric and asymmetric parts is depicted in Fig. 3. Arbitrary units have been used for functions $\beta'_{\text{II},\perp,\text{v}}$ in order to highlight the angular dependence of $\mathcal{S}$ and $\mathcal{A}$. The color code represents $\mathcal{S}$ in Figs. 3(a)–3(c) and $\mathcal{A}$ in Figs. 3(d)–3(g). Here, typical magnetic parameters of CoFeB/MgO have been used, namely $M_s = 950$ kA/m, $\gamma = 29.5$ GHz/T, $\mu_0 H^0 = 2$ T, and $\mu_0 H^0_s = 1$ T. Also, the demagnetizing factors associated with the principal axes are $N_a = 0.014$, $N_b = 0.040$, and $N_c = 0.946$, where a, b, and c stand for the long, short, and normal axis, respectively. By distinguishing the ip, oop, and full magnetization reversal processes [see Fig. 3(a)], it is observed that VCMA induces a change of sign by depending on the nature of the magnetization rotation. Namely, the symmetric part changes its sign under ip and oop magnetization reversal in such a way that a full reversion of the magnetization recovers the same symmetric function. In the asymmetric part $\mathcal{A}$ [see Fig. 3(d)] a different situation is obtained, since this part of the line shape changes its sign under ip and full magnetization reversal, while it remains unaltered when the magnetization reverses out-of plane. Thus, the role of VCMA over functions $\mathcal{S}$ and $\mathcal{A}$ is clearly established. On the other side, it is noted that FLT is important only in the asymmetric part. Indeed, the FLT does not affect the symmetric part, while the ipSTT influences both functions $\mathcal{S}$ and $\mathcal{A}$, but its contribution to the asymmetric part is very weak for realistic magnetic parameters. In Fig. 3(e)

TABLE I. Summary of the influence of ipSTT, FLT, and VCMA on the FMR spectral line shape on MTJs.

Geometry of the system		Spectral line shape effects	
		Symmetric part	Asymmetric part
p parallel to the long axis	In-plane component of **m** parallel to the long axis	ipSTT	FLT, VCMA
	In-plane component of **m** parallel to the short axis	ipSTT, VCMA	FLT
	m in the film's plane	ipSTT	FLT
p perpendicular to the film's plane	**m** at arbitrary polar angle	ipSTT	FLT, VCMA

it is noted that there is a change of sign due to ipSTT when the azimuthal angle changes from φ to $\varphi \pm 90°$; and when the polar angle changes from θ to $180° - \theta$. The peculiarity of this effect is that it becomes null for typical configurations, such as mentioned in Secs. III A and III B. Therefore, if the ipSTT dominates, its role on the asymmetric part can be observed as long as the magnetization is in a canted state with respect to the main axes.

If the VCMA dominates, as mentioned above, it is expected that the spectral line shape changes its sign when the azimuthal angle changes from φ to $\varphi \pm 180°$, i.e., under an in-plane magnetization reversal. In Fig. 4 the line shape L_s is depicted as a function of φ, θ, and ω/ω_r at null STT. In Fig. 4(a), the angle θ is kept at 50°, while φ is varied. Here the response is dominated by the asymmetric part $\mathcal{A}$ and it is zero when $\varphi = 90°$, as shown in Eq. (14b). On the other side, by keeping $\varphi = \pm 90°$, one can see that the symmetric part $\mathcal{S}$ becomes important and it also changes its sign, as depicted in Fig. 4(b). Thus, it is demonstrated that the change of sign in the spectral line shape, under the variation from φ to $\varphi \pm 180°$ (ip magnetization reversal), can be considered as a fingerprint of the VCMA, such as was previously reported for some specific geometries [18,22]. In addition to the change of sign under an ip magnetization reversal, the role of the out-of-plane angle is clearly described, in the sense that it is necessary to distinguish between the nature of the reversion to detect the influence of VCMA, as discussed above.

Table I shows a summary of the angular dependence of the spectral line shape for typical geometrical configurations. In each case, the effect of VCMA field, ipSTT, and FLT is identified and hence, a systematic analysis of these results can

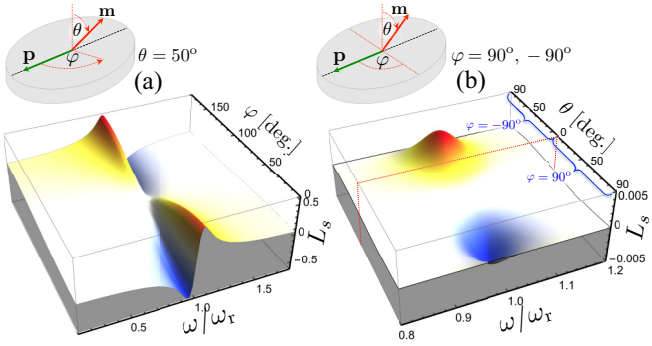

FIG. 4. Line shape as a function of φ, θ, and ω/ω_r. In (a) the angle θ is kept fixed at 50° and the azimuthal angle φ is varied from 0 up to 180°. In (b) the angle φ is kept fixed at $\pm$ 90°, while the angle θ is varied from 0 up to 90°. Here $\lambda = 0.1\omega_r$ and null STTs are assumed.

be used as a guide for experimentalists who are interested in studying MTJs with varied geometrical configurations, since these findings allow discriminating the different contributions induced by the combined action of VCMA and STT. When **p** is perpendicular to the film's plane, VCMA mainly affects the asymmetric part, this behavior also agrees with recent experimental results observed on CoFeB/MgO perpendicular MTJs [42].

IV. SUMMARY

Analytical expressions for the spectral ferromagnetic resonance line shape have been theoretically derived when the excitation is induced by the combined action of spin-transfer torque and voltage-controlled magnetic anisotropy. Explicit expressions for the symmetric and asymmetric parts are obtained and they can serve as a guide for discriminating the role of the voltage-controlled magnetic anisotropy and the spin-transfer torque effects in the ferromagnetic resonance response of magnetic tunnel junctions. Overall, the results are in very good concordance with recent experimental results, which corroborates the reliability of the theoretical findings. By taken into account the generality of the results, it is demonstrated that the change of sign upon an in-plane magnetization reversal is completely due to VCMA and thus, this effect can be considered as a fingerprint of the voltage-controlled magnetic anisotropy phenomenon. Besides, it is also shown that VCMA induces a change of sign in the symmetric part for the in-plane and out-of-plane magnetization reversal; while the asymmetric parts change its sign under a full and in-plane reversion of the magnetization. The proposed theory allows accessing to a better understanding of the physics behind ferromagnetic resonance phenomena in magnetic tunnel junctions, providing simple and useful expressions that may encourage further experimental studies in nanostructured systems and promote potential applications in STT+VCMA-based devices.

ACKNOWLEDGMENTS

C.G.-F. acknowledges the financial support received by FONDECYT Grant No. 3170908. R.A.G. acknowledges financial support from CONICYT PAI/ACADEMIA, under Contract 79140033. This work was also supported by FONDECYT under Grants No. 1161403 and No. 1140552 and Basal Program for Centers of Excellence CONICYT, Grant FB0807 CEDENNA, and Grant FB0821, CCTVal.

APPENDIX: EXPLICIT EXPRESSIONS FOR $H_{\eta\eta'}$ AND $\Omega_{\eta\eta'}$

The elements $H_{\eta\eta'}$ can be derived from the magnetic energy density, which up to second order in the spin deviation

becomes [8]

$$\epsilon = \epsilon_0 + \sum_{\eta} \Lambda_\eta m_\eta + \frac{1}{2M_s} \sum_{\eta\eta'} H_{\eta\eta'} m_\eta m_{\eta'}, \tag{A1}$$

where ϵ_0 can be ignored, since it does not affect either the equilibrium state or the dynamic behavior. Thus, after some algebra the coefficients $H_{\eta\eta'}$ are

$$H_{xx} = \mu_0 H_z^0 + M_e \cos^2\theta + \mu_0 M_s f_x, \tag{A2a}$$

$$H_{yy} = \mu_0 H_z^0 + M_e \cos 2\theta - \mu_0 M_s f_y, \tag{A2b}$$

$$H_{xy} = \mu_0 M_s (N_a - N_b) \cos\theta \cos\varphi \sin\varphi. \tag{A2c}$$

Here $H_z^0 = H^0[\sin\theta \sin\theta_h \cos(\varphi - \varphi_h) + \cos\theta \cos\theta_h]$ and $M_e = \mu_0 H_s^0 - \mu_0 N_c M_s$, with N_η being the demagnetizing factors of the elliptical structure, also,

$$f_x = \frac{N_a}{4}[1 + 3\cos 2\varphi + 2\sin^2\varphi \cos 2\theta] + N_b(\sin^2\varphi - \sin^2\theta \cos^2\varphi)$$

and $f_y = -(N_a \sin^2\varphi + N_b \cos^2\varphi)\cos 2\theta$. By taking into account the definitions of $H_{\eta,\eta'}$, the elements $\Omega_{\eta\eta'}$ are

$$\Omega_{xy} = \gamma(I_{dc}\beta'_{\shortparallel} p_z - H_{xy}), \tag{A3a}$$

$$\Omega_{yy} = \gamma[-H_{yy} + I_{dc}(\beta'_{\perp} p_z + \beta'_v \cos 2\theta)], \tag{A3b}$$

$$\Omega_{xx} = \gamma[H_{xx} - I_{dc}(\beta'_{\perp} p_z + \beta'_v \cos^2\theta)], \tag{A3c}$$

$$\Omega_{yx} = \gamma(H_{xy} + I_{dc}\beta'_{\shortparallel} p_z). \tag{A3d}$$

[1] J. Slonczewski, J. Magn. Magn. Mater. **159**, L1 (1996).
[2] L. Berger, Phys. Rev. B **54**, 9353 (1996).
[3] S. Zhang and Z. Li, Phys. Rev. Lett. **93**, 127204 (2004).
[4] J. S. Moodera, L. R. Kinder, T. M. Wong, and R. Meservey, Phys. Rev. Lett. **74**, 3273 (1995).
[5] T. Miyazaki and N. Tezuka, J. Magn. Magn. Mater. **139**, L231 (1995).
[6] S. S. P. Parkin, C. Kaiser, A. Panchula, P. M. Rice, B. Hughes, M. Samant, and S.-H. Yang, Nat. Mater. **3**, 862 (2004).
[7] Z. Zeng, G. Finocchio, and H. Jiang, Nanoscale **5**, 2219 (2013).
[8] C. Gonzalez-Fuentes, R. A. Gallardo, and P. Landeros, Appl. Phys. Lett. **107**, 142402 (2015).
[9] F. Matsukura, Y. Tokura, and H. Ohno, Nat. Nano **10**, 209 (2015).
[10] K. Nakamura, R. Shimabukuro, Y. Fujiwara, T. Akiyama, T. Ito, and A. J. Freeman, Phys. Rev. Lett. **102**, 187201 (2009).
[11] K. Nakamura, R. Shimabukuro, T. Akiyama, T. Ito, and A. J. Freeman, Phys. Rev. B **80**, 172402 (2009).
[12] T. Maruyama, Y. Shiota, T. Nozaki, K. Ohta, N. Toda, M. Mizuguchi, A. A. Tulapurkar, T. Shinjo, M. Shiraishi, S. Mizukami, Y. Ando, and Y. Suzuki, Nat. Nano **4**, 158 (2009).
[13] Y. Shiota, T. Maruyama, T. Nozaki, T. Shinjo, M. Shiraishi, and Y. Suzuki, Appl. Phys. Express **2**, 063001 (2009).
[14] K. Nakamura, T. Akiyama, T. Ito, M. Weinert, and A. J. Freeman, Phys. Rev. B **81**, 220409 (2010).
[15] T. Nozaki, Y. Shiota, M. Shiraishi, T. Shinjo, and Y. Suzuki, Appl. Phys. Lett. **96**, 022506 (2010).
[16] M. Endo, S. Kanai, S. Ikeda, F. Matsukura, and H. Ohno, Appl. Phys. Lett. **96**, 212503 (2010).
[17] Y. Shiota, S. Murakami, F. Bonell, T. Nozaki, T. Shinjo, and Y. Suzuki, Appl. Phys. Express **4**, 043005 (2011).
[18] J. Zhu, J. A. Katine, G. E. Rowlands, Y.-J. Chen, Z. Duan, J. G. Alzate, P. Upadhyaya, J. Langer, P. K. Amiri, K. L. Wang, and I. N. Krivorotov, Phys. Rev. Lett. **108**, 197203 (2012).
[19] T. Nozaki, Y. Shiota, S. Miwa, S. Murakami, F. Bonell, S. Ishibashi, H. Kubota, K. Yakushiji, T. Saruya, A. Fukushima, S. Yuasa, T. Shinjo, and Y. Suzuki, Nat. Phys. **8**, 491 (2012).
[20] W.-G. Wang, M. Li, S. Hageman, and C. L. Chien, Nat. Mater. **11**, 64 (2012).
[21] Y. Shiota, T. Nozaki, F. Bonell, S. Murakami, T. Shinjo, and Y. Suzuki, Nat. Mater. **11**, 39 (2012).
[22] Y. Shiota, S. Miwa, S. Tamaru, T. Nozaki, H. Kubota, A. Fukushima, Y. Suzuki, and S. Yuasa, J. Magn. Magn. Mater. **400**, 159 (2016).
[23] K. Miura, S. Yabuuchi, M. Yamada, M. Ichimura, B. Rana, S. Ogawa, H. Takahashi, Y. Fukuma, and Y. Otani, Sci. Rep. **7**, 42511 (2017).
[24] K.-J. Lee, A. Deac, O. Redon, J.-P. Nozieres, and B. Dieny, Nat. Mater. **3**, 877 (2004).
[25] A. M. Deac, A. Fukushima, H. Kubota, H. Maehara, Y. Suzuki, S. Yuasa, Y. Nagamine, K. Tsunekawa, D. D. Djayaprawira, and N. Watanabe, Nat. Phys. **4**, 803 (2008).
[26] C. Wang, Y.-T. Cui, J. A. Katine, R. A. Buhrman, and D. C. Ralph, Nat. Phys. **7**, 496 (2011).
[27] K. Bernert, V. Sluka, C. Fowley, J. Lindner, J. Fassbender, and A. M. Deac, Phys. Rev. B **89**, 134415 (2014).
[28] X. Zhang, C. Wang, Y. Liu, Z. Zhang, Q. Y. Jin, and C.-G. Duan, Sci. Rep. **6**, 18719 (2016).
[29] A. A. Tulapurkar, Y. Suzuki, A. Fukushima, H. Kubota, H. Maehara, K. Tsunekawa, D. D. Djayaprawira, N. Watanabe, and S. Yuasa, Nature (London) **438**, 339 (2005).
[30] Y. Gui, L. Bai, and C. Hu, Sci. China Phys. Mech. Astron. **56**, 124 (2013).
[31] J. C. Sankey, Y.-T. Cui, J. Z. Sun, J. C. Slonczewski, R. A. Buhrman, and D. C. Ralph, Nat. Phys. **4**, 67 (2008).
[32] H. Kubota, A. Fukushima, K. Yakushiji, T. Nagahama, S. Yuasa, K. Ando, H. Maehara, Y. Nagamine, K. Tsunekawa, D. D. Djayaprawira, N. Watanabe, and Y. Suzuki, Nat. Phys. **4**, 37 (2008).
[33] X. Fan, R. Cao, T. Moriyama, W. Wang, H. W. Zhang, and J. Q. Xiao, Appl. Phys. Lett. **95**, 122501 (2009).
[34] M. R. Pufall, W. H. Rippard, S. E. Russek, and E. R. Evarts, Phys. Rev. B **86**, 094404 (2012).
[35] A. M. Sahadevan, K. Gopinadhan, C. S. Bhatia, and H. Yang, Appl. Phys. Lett. **101**, 162404 (2012).
[36] M. A. Subramanian, R. D. Shannon, B. H. T. Chai, M. M. Abraham, and M. C. Wintersgill, Phys. Chem. Miner. **16**, 741 (1989).

[37] P. Landeros, R. A. Gallardo, O. Posth, J. Lindner, and D. L. Mills, Phys. Rev. B **81**, 214434 (2010).
[38] J. C. Sankey, P. M. Braganca, A. G. F. Garcia, I. N. Krivorotov, R. A. Buhrman, and D. C. Ralph, Phys. Rev. Lett. **96**, 227601 (2006).
[39] M. Harder, Y. Gui, and C.-M. Hu, Phys. Rep. **661**, 1 (2016).
[40] N. Mecking, Y. S. Gui, and C.-M. Hu, Phys. Rev. B **76**, 224430 (2007).
[41] J. C. Slonczewski, Phys. Rev. B **39**, 6995 (1989).
[42] H. Mazraati, T. Q. Le, A. A. Awad, S. Chung, E. Hirayama, S. Ikeda, F. Matsukura, H. Ohno, and J. Åkerman, Phys. Rev. B **94**, 104428 (2016).